

PAPER • OPEN ACCESS

Particle decay of astrophysically-important ^{19}Ne levels

To cite this article: D W Bardayan *et al* 2019 *J. Phys.: Conf. Ser.* **1308** 012004

View the [article online](#) for updates and enhancements.



IOP | ebooks™

Bringing together innovative digital publishing with leading authors from the global scientific community.

Start exploring the collection—download the first chapter of every title for free.

Particle decay of astrophysically-important ^{19}Ne levels

D W Bardayan^{1,2}, K A Chipps^{2,3,4}, S Ahn^{3,5}, J C Blackmon⁶, U Greife⁴, K L Jones³, A Kontos⁵, R L Kozub⁷, L Linhardt⁶, B Manning⁸, M Matos^{2,3}, P D O'Malley¹, S Ota⁸, S D Pain², W A Peters^{2,3}, S T Pittman^{2,3}, A Sachs³, K T Schmitt^{2,3}, M S Smith² and P Thompson^{2,3}

¹ Dept. of Physics, University of Notre Dame, Notre Dame, IN 46556, USA

² Physics Division, Oak Ridge National Lab, Oak Ridge, TN 37831, USA

³ Dept. of Physics and Astronomy, University of Tennessee, Knoxville, TN 37996 USA

⁴ Dept. of Physics, Colorado School of Mines, Golden, CO 80401, USA

⁵ National Superconducting Cyclotron Lab, Michigan State University, East Lansing, MI 48824, USA

⁶ Dept. of Physics and Astronomy, Louisiana State University, Baton Rouge, LA 70803, USA

⁷ Dept. of Physics, Tennessee Technological University, Cookeville, TN 38505, USA

⁸ Dept. of Physics and Astronomy, Rutgers University, Piscataway, NJ 08854, USA

E-mail: danbardayan@nd.edu

Abstract. The $^{15}\text{O}(\alpha, \gamma)^{19}\text{Ne}$ reaction is an important trigger reaction leading to the rapid proton (rp) capture process in X-ray bursts. The primary uncertainty in determining its astrophysical rate is the uncertain α branching ratios of levels near $E_x = 4.1$ MeV in ^{19}Ne . These states have been populated in a study of the $^{20}\text{Ne}(p, d)^{19}\text{Ne}$ reaction, and α branching ratios are reported in this manuscript.

1. Introduction

The $^{15}\text{O}(\alpha, \gamma)^{19}\text{Ne}$ reaction triggers the rp -process in X-ray bursts and sets the stage for maximum light emission at the peak of the burst. The central role the $^{15}\text{O}(\alpha, \gamma)^{19}\text{Ne}$ reaction rate plays was recently demonstrated from its large effect on X-ray burst light curves [1]. In fact, if the $^{15}\text{O}(\alpha, \gamma)^{19}\text{Ne}$ reaction rate is near the lower limit of current estimates, models would even fail to predict X-ray burst explosions [2].

The temperatures at which the reaction rate becomes faster than the ^{15}O β decay is determined by the properties of ^{19}Ne levels near the α -emission threshold at 3.529 MeV. Of particular interest are levels at 4034 keV ($J^\pi = 3/2^+$), 4142 keV ($7/2^-$), and 4200 keV ($9/2^-$) [3]. While the levels energies are well known, it was only recently that the spins of the two higher-energy levels were clarified [4]. In addition, the lifetimes of these levels have been measured using Doppler-shift attenuation methods [5, 6]. The last remaining quantity that needs to be determined in order to calculate the $^{15}\text{O}(\alpha, \gamma)^{19}\text{Ne}$ rate are the α -branching ratios, $B_\alpha = \Gamma_\alpha/\Gamma$ since the α widths are expected to be much smaller than the γ widths. Multiple attempts have been made in the past to measure the α -branching ratios [3, 7, 8, 9] with one [3] reporting branching ratios of $B_\alpha = (2.9 \pm 2.1) \times 10^{-4}$ for the 4034-keV level and $B_\alpha = (1.2 \pm 0.5) \times 10^{-3}$ for



the combined 4142- and 4200-keV levels, which could not be resolved. All of the other previous measurements did not reach the sensitivity level required to measure the small α branching ratios near threshold. In this manuscript, a new analysis of $^{20}\text{Ne}(p, d)^{19}\text{Ne}$ data [10] is reported in order to study the α -branching ratios of astrophysically-important ^{19}Ne levels affecting estimates of the $^{15}\text{O}(\alpha, \gamma)^{19}\text{Ne}$ astrophysical reaction rate.

2. Experiment

A full description of the JENSA gas-jet target is given in Ref. [11]. Briefly, high pressure gas (~ 16000 Torr) is injected through a Laval nozzle to form a dense jet of gas approximately 4 mm wide. After passing through the target region, the gas is received, compressed, and recirculated back through the target with the aid of multiple stages of pumping and compression. The interaction point of the beam with the gas jet is surrounded by arrays of silicon detectors such as SIDAR [12], the Oak Ridge Rutgers University Barrel Array (ORRUBA) [13], and SuperORRUBA [14]. The effective areal density of the jet was estimated by measuring the energy loss of α particles emitted from a ^{244}Cm source and was found to be $\sim 4 \times 10^{18}$ Ne atoms/cm². Precise knowledge of the target density was not necessary for this analysis as the primary goal was to measure the fraction of the time that a deuteron populating a given ^{19}Ne state was accompanied by a decay α particle.

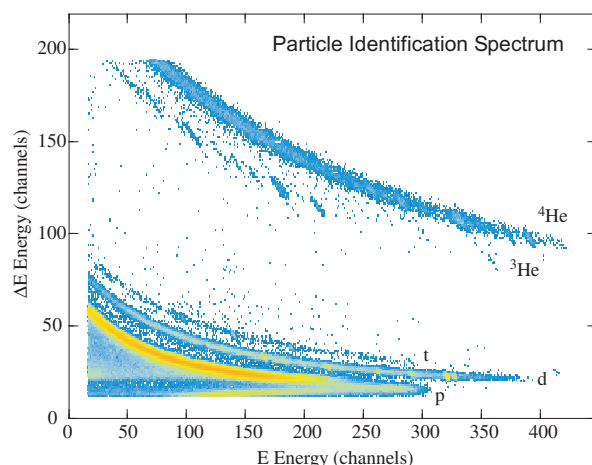


Figure 1. A particle identification spectrum from one of the SIDAR telescopes. The deuterons of interest are cleanly separated from other particle groups.

30-MeV proton beams were accelerated at the Holifield Radioactive Ion Beam Facility [15] and used to bombard ^{nat}Ne gas-jet targets. The beam was tuned and focused to a spot size of 2-3 mm at an optically-aligned retractable scintillating phosphor ensuring spatial overlap with the JENSA gas jet. Reaction ejectiles were detected and identified using elements of the SIDAR configured in telescope mode with 65- μm -thick ΔE detectors being backed by 1000- μm -thick E detectors and covering laboratory angles between $18^\circ - 53^\circ$. A particle-identification spectrum from the experiment is plotted in Fig. 1. The various observed particle groups ($p, d, t, ^3\text{He}$, and ^4He ions) were well separated using this energy-loss technique. The most intense group (10-20 kHz) arose from elastically-scattered protons, which were preferentially suppressed from the data acquisition by applying a hardware energy threshold to the ΔE detector signals.

The observed deuteron spectrum produced at 29° after bombardment with 3 nA proton beams for 15 hours is shown in Fig. 2. The spectrum shows excellent correspondence with known ^{19}Ne levels. A few deuteron peaks were observed from the $^{22}\text{Ne}(p, d)^{21}\text{Ne}$ reaction (labeled as ^{22}Ne in Fig. 2), but those were easily identified by their differing kinematic shifts. All other peaks correspond to known states in ^{19}Ne . The relatively smooth background between the peaks in

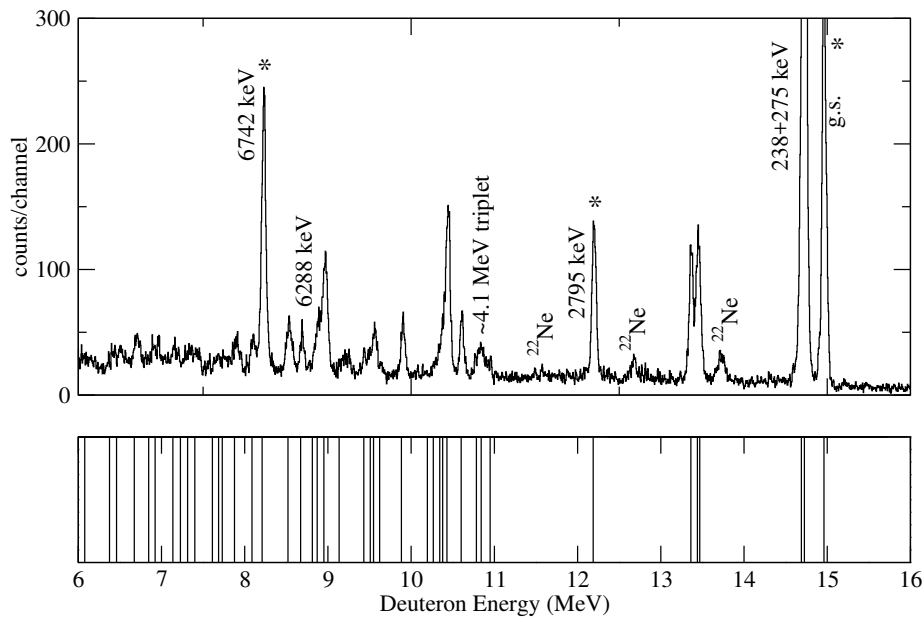


Figure 2. The top panel shows observed deuteron energy spectrum at 29° while the bottom panel shows the expected energies for the population of known levels in the $^{20}\text{Ne}(p,d)^{19}\text{Ne}$ reaction at the same angle and a bombarding energy of 30 MeV. Peaks labeled with stars were used for energy calibration.

the spectrum arises from effects such as incomplete charge collection in the silicon detectors and random coincidences in the deuteron gate arising primarily from pileup of elastically-scattered proton pulses. The deuteron energy calibration was performed using the strongly populated, isolated, and well-known levels at $E_x = 0$, 2795, and 6742 keV. Multiple states above the α and p thresholds were observed including the triplet of states near 4.1 MeV important for determining the $^{15}\text{O}(\alpha, \gamma)^{19}\text{Ne}$ reaction rate.

To search for α -decay events originating from the decay of excited ^{19}Ne levels, a spectrum was constructed of coincident charged particles that hit any other telescope besides the one in which the deuteron was detected. This condition was implemented to avoid confusing decay events with events that might mimic decay such as crosstalk in a single detector. The coincidence window was set in hardware to $4 \mu\text{s}$ for this experiment, and the expected α energies (> 500 keV) were above the hardware threshold of 300 keV. If charged particles were detected from the decay of excited states, there should be a clear correlation between the decay energies and the excited state populated (i.e., the lower deuteron energies corresponding to population of higher excited states result in higher charged-particle decay energies). The spectrum constructed from this coincidence requirement is plotted in Fig. 3. A clear band is visible showing the correlation expected for decay α events with the lowest energy α particles corresponding to deuterons populating states at the α threshold. The deuteron energy spectrum for events occurring within this decay band are plotted in Fig. 4.

In order to extract the α -branching ratios for populated ^{19}Ne levels, the random coincidence background first needed to be estimated. Random coincidences mostly arise as a result of the relatively high elastically-scattered proton rate ($\sim 10 - 20$ Hz) in the silicon detectors as evidenced in Fig. 3 by vertical streaks at fixed deuteron energies populating bound ^{19}Ne levels (e.g., near the deuteron energy channel of 370). This random coincidence background was most intense at the lowest α energies. To estimate the probability for a random coincidence, the

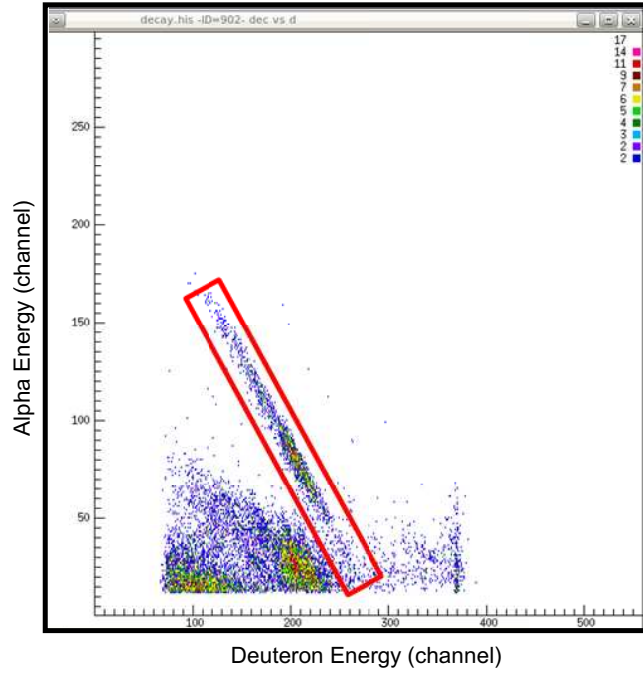


Figure 3. Decay energies plotted as a function of deuteron energies. Deuterons populating unbound ^{19}Ne levels show the expected correlation with decay α energies as indicated by the gate in this spectrum.

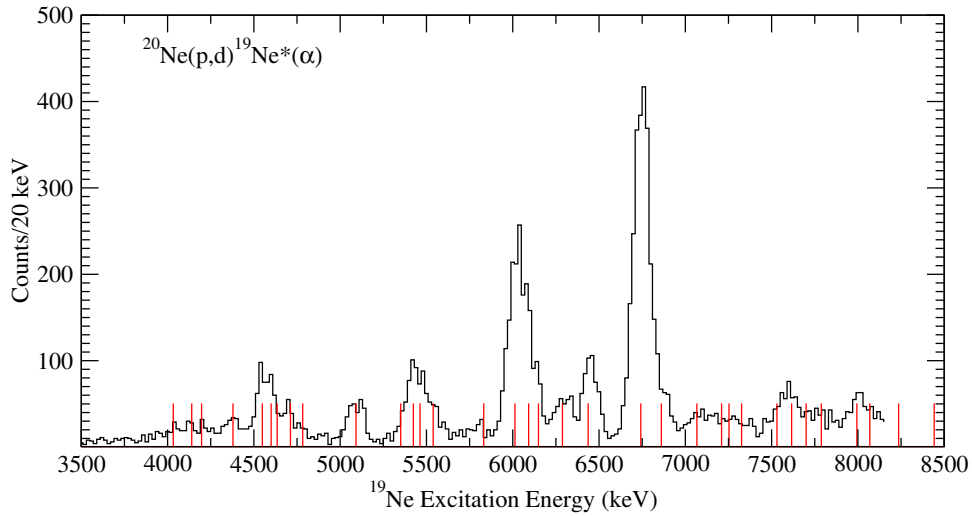


Figure 4. The deuteron energy spectrum in coincidence with decay α particles. As expected, decay α events are observed to start at the α threshold except for random coincidences producing a continuous background. The vertical lines indicate the previously-measured ^{19}Ne excitation energies. Small peaks are observed for the important 4.1-MeV triplet of states.

number of events were counted in coincidence with deuterons populating the bound ^{19}Ne levels at 0, 235, and 275 keV. The probability was observed to be as high as 0.8% between α energies of 400-800 keV and decreased to 0.005% between 3000-4000 keV.

The coincidence efficiency of the detector system was determined by considering the decay of ^{19}Ne levels known to decay with 100% α -branching ratios. The levels considered for this analysis were the 6742/6861-keV doublet with α widths 1000 times larger than any other decay widths [16]. After comparing the number of counts observed in this double peak in Figs. 2 and 4 and

subtracting the random coincidences ($\sim 0.01\%$), the coincidence efficiency was determined to be $(7.4 \pm 0.2)\%$.

Using these values for the random coincidence probabilities and the coincidence efficiency, the α branching ratios for other levels could be determined assuming isotropic distributions in the ^{19}Ne rest frame. The preliminary branching ratios measured from this work are shown in Table 1. The quoted uncertainties are statistical in nature and do not include the possible effects of anisotropic α distributions. At this stage, it has not been possible to extract α branching ratios for the ~ 4.1 -MeV triplet of states as the random coincidence background is too large. It is hoped that through further analysis of the data, cleaner coincidence requirements can be implemented to further reduce this random coincidence background.

Table 1. Preliminary α branching ratios measured in this work. The excitation energies are taken from Ref. [10].

^{19}Ne Level	B_α (present)	B_α [9]	B_α [8]	B_α [7]
6.438(2) MeV	1.1 ± 0.1			
6.282(3) MeV	1.1 ± 0.2			
6.0-MeV triplet	1.00 ± 0.4			
5.539(9) MeV	0.88 ± 0.05			
5.090(6) MeV	0.61 ± 0.06	0.8 ± 0.1	0.90 ± 0.06	0.90 ± 0.09
4.371(3) MeV	$< 3 \times 10^{-2}$	0.016 ± 0.005	$< 3.9 \times 10^{-3}$	0.044 ± 0.032

3. Conclusions

Data from the $^{20}\text{Ne}(p,d)^{19}\text{Ne}$ reaction [10] have been re-analyzed to search for accompanying α decay. The α -decay branching ratios are important for constraining the astrophysical $^{15}\text{O}(\alpha,\gamma)^{19}\text{Ne}$ reaction rate. Branching ratios for higher-lying levels have been extracted but the sensitivity has not yet been reached in order to extract ratios for the most important 4.1-MeV triplet of ^{19}Ne levels. Further analysis of the data is in progress.

This work was supported in part by the U.S. Department of Energy under Contract Nos. DE-FG02-10ER41704 and DE-FG02-93ER40789 (CSM), DE-FG52-08NA28552 (Rutgers), DE-FG02-96ER40983 (UTK), DE-FG02-96ER40955 (TTU), DE-AC05-00OR22725 (ORNL), and the National Science Foundation under Contract Nos. PHY-1419765 (Notre Dame) and PHY-0822648 (JINA).

References

- [1] J. L. Fisker, J. Gorres, M. Wiescher, *Astrophys. J.* **50**, 332 (2006).
- [2] R. H. Cyburt, A. M. Amthor, A. Heger, E. Johnson, L. Keek, Z. Meisel, H. Schatz, K. Smith, *Astrophys. J.* **830**, 55 (2016).
- [3] W. P. Tan, J. L. Fisker, J. Gorres, M. Couder, M. Wiescher, *Phys. Rev. Lett.* **98**, 242503 (2007).
- [4] M. R. Hall *et al.*, *Phys. Rev. C* (in press).
- [5] W. P. Tan *et al.*, *Phys. Rev. C* **72**, 041302(R) (2005).
- [6] R. Kanungo *et al.*, *Phys. Rev. C* **74**, 045803 (2006).
- [7] P. V. Magnus *et al.*, *Nucl. Phys. A* **506**, 332 (1990).
- [8] B. Davids *et al.*, *Phys. Rev. C* **67**, 065808 (2003).
- [9] K. E. Rehm *et al.*, *Phys. Rev. C* **67**, 065809 (2003).
- [10] D. W. Bardayan *et al.*, *Phys. Lett. B* **751**, 311 (2015).
- [11] K. A. Chipps *et al.*, *Nucl. Instrum. Meth. Phys. Res. A* **763**, 553 (2014).
- [12] D. W. Bardayan *et al.*, *Phys. Rev. Lett.* **83** (1999) 45.
- [13] S. D. Pain *et al.*, *Nucl. Instr. and Meth. in Phys. Res. B* **261** (2007) 1122.

- [14] D. W. Bardayan *et al.*, Nucl. Instr. and Meth. in Phys. Res. A **711** (2013) 160.
- [15] J. R. Beene *et al.*, J. Phys. G: Nucl. Part. Phys. **38** (2011) 024002.
- [16] C. Akers *et al.*, Phys. Rev. C. **94**, 065803 (2016).